

Supporting Information for

Cholate-conjugated cationic polymers for regulation of actin dynamics

Subhasish Sahoo,^{a,#} Ipsihita Maiti,^{b,#} Arkayan Laha,^c Rumi De,^{c,*} Sankar Maiti,^{b,*} Priyadarsi De^{a,*}

^aPolymer Research Centre and Centre for Advanced Functional Materials, Department of Chemical Sciences, ^bDepartment of Biological Sciences, ^cDepartment of Physical Sciences, Indian Institute of Science Education and Research Kolkata, Mohanpur - 741246, Nadia, West Bengal, India

[#]These authors contributed equally to this work.

*Corresponding authors: Emails: rumi.de@iiserkol.ac.in (RD), spm@iiserkol.ac.in (SM), p_de@iiserkol.ac.in (PD)

Materials and Methods

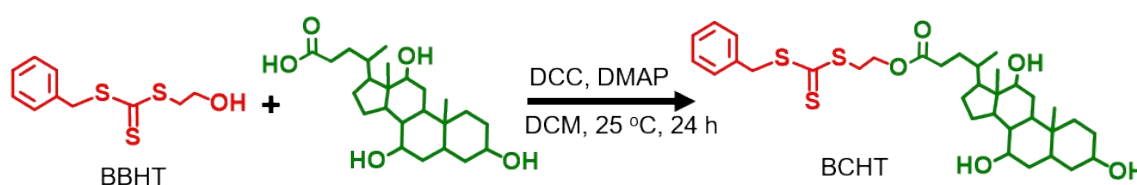
Materials. Cholic acid (CA, $\geq 98\%$), Boc-L-leucine (Boc-L-Leu-OH, 99%), 2-hydroxyethyl methacrylate (HEMA, 97%), 4-dimethylaminopyridine (DMAP, 99%), dicyclohexylcarbodiimide (DCC, 99%), and anhydrous *N,N*-dimethylformamide (DMF, 99.9%) were purchased from Sigma and used without any further purification. Boc-L-alanine (Boc-L-Ala-OH, 99%), Boc-L-phenylalanine (Boc-L-Phe-OH, 99%), and the Boc-protecting agent trifluoroacetic acid (TFA, 99.5%) were obtained from Sisco Research Laboratories Pvt. Ltd, India and used as received. Polyethylene glycol methyl ether

methacrylate (PEGMA, average molecular weight = 300 g/mol) was received from Sigma (99%) and purified before polymerization by passing through a basic alumina column. The initiator 2,2'-azobisisobutyronitrile (AIBN, Sigma, 98%) was recrystallized twice from methanol. The CA conjugated vinyl monomer, 2-(methacryloyloxy)-ethyl cholate (MAECA) was synthesized by the coupling reaction of CA with HEMA in the presence of DCC and DMAP as reported previously.¹ The NMR solvents such as chloroform-*d* (CDCl₃, 99.8% D) and dimethyl sulphoxide-*d*₆ (DMSO-*d*₆, 99.8% D) were obtained from Cambridge Isotope Laboratories, Inc., USA. The dialysis membrane bag (Spectra/Por 7, 2 kDa molecular weight cut-off) was purchased from Spectrum Laboratories, Inc. The solvents like hexanes, tetrahydrofuran (THF), and dichloromethane (DCM) were purified by following the general procedure.² A solution of Dulbecco's Modified Eagle Medium (DMEM, Gibco, Thermo Fisher Scientific) containing 10% fetal bovine serum (Gibco) and penicillin-streptomycin (Hyclone, Thermo Scientific) was prepared for growing the HeLa cells for cytotoxicity assay. The formazan crystals produced from 3-(4,5-dimethylthiazol-2-yl)-2,5-diphenyltetrazolium bromide (MTT, USB Corporation) cellular treatment was dissolved in dimethyl sulphoxide (DMSO, 99.9%, cell culture grade, Amresco). Alexa 488 Phalloidin (Invitrogen) was used for *in vitro* microscopy of actin filaments.

Instrumentation. The molecular weight of the polymers and their dispersity (*D*) were determined by size exclusion chromatography (SEC) using poly(methyl methacrylate) (PMMA) standards (conventional calibration) in DMF with a flow rate of 0.8 mL/min at 40 °C. The instrument consists of a Waters Model 1515 HPLC pump, one PolarGel-M guard column (50 × 7.5 mm), two PolarGel-M analytical columns (300 × 7.5 mm), and a Waters 2414 refractive index (RI) detector. The ¹H NMR spectroscopy was acquired both in a JEOL-FT NMR-AL 400 MHz spectrometer and a Bruker Avance^{III} 500 MHz spectrometer. High

resolution mass spectrometry (HR-MS) was recorded in maXis impact (Bruker) mass spectrometer using positive mode electrospray ionization. The UV-Vis spectroscopic measurements were conducted on a U-4100 spectrophotometer HITACHI UV-Vis spectrometer with a scan rate of 240 nm min⁻¹. Fluorescence emission spectra were recorded on a Fluorescence spectrometer (Horiba Jobin Yvon, Fluoromax-4). Fluorescence of pyrene actin was recorded at 407 nm emission wavelength through excitation at 365 nm wavelength at 25 °C in a fluorescence spectrophotometer (QM40, Photon Technology International, Lawrenceville, NJ). Hydrodynamic size distributions and zeta potential values were measured in a Malvern Nano Zetasizer dynamic light scattering (DLS) instrument, that was equipped with a helium-neon laser operational at a 633 nm wavelength and at a detection angle of 173° at room temperature.

Synthesis of *S*-benzyl *S'*-hydroxyethylthiocarbonate (BBHT) and *S*-benzyl *S'*-(cholyloxyethylthiocarbonate (BCHT) chain transfer agents (CTAs). BBHT was prepared following an earlier literature procedure.³ The cholate-based CTA BCHT was synthesized by the Steglich esterification procedure from BBHT as shown in Scheme S1 and characterized by ¹H NMR (Fig. S1) and HR-MS spectroscopy (Fig. S2).



Scheme S1. Synthesis of BCHT from BBHT using DCC/DMAP esterification process (Yield = 82%).

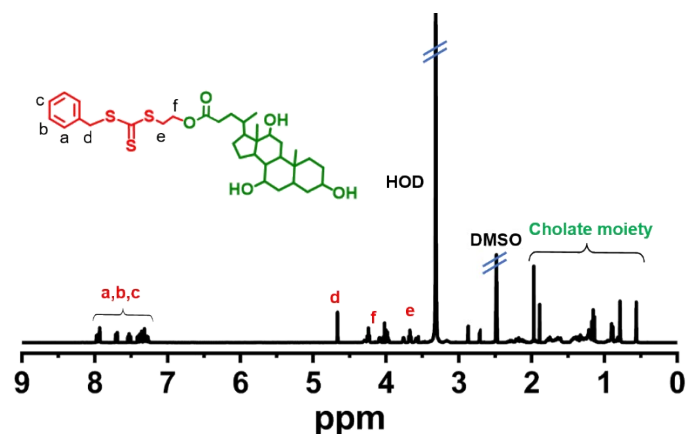


Fig. S1 ^1H NMR spectrum of BCHT in $\text{DMSO-}d_6$ solvent.

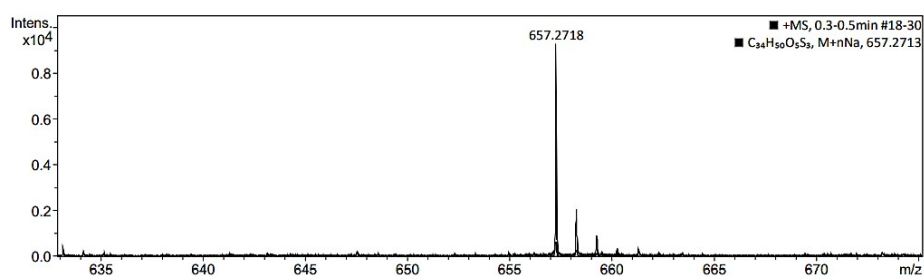


Fig. S2 HR-MS spectrum of BCHT. Observed m/z for $[\text{M} + \text{Na}]^+ = 657.2718$, Calculated m/z for $[\text{M} + \text{Na}]^+ = 657.2698$.

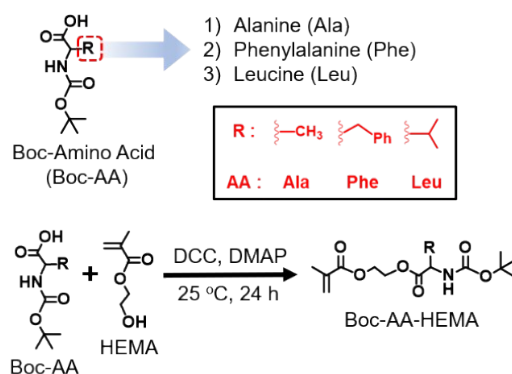


Fig. S3 Synthesis of different amino acid (AA: Ala-, Phe-, and Leu-) derived Boc-protected monomers Boc-AA-HEMA, using DCC/DMAP esterification process.

Turbidity assay. The pH-responsive phase transition behaviour of the deprotected polymers was investigated by measuring the turbidity change *via* UV-visible spectroscopy. 2 mg of each

polymer was dissolved in 1 mL of water and placed in a cuvette to monitor the transmittance percentage (%*T*) value at a wavelength of 500 nm with varying pH at room temperature. The pH at which the %*T* value is reduced to 50% is termed as phase transition pH.

Cytotoxicity assay. The cellular toxicity of the deprotected polymers was analysed through MTT assay with *in vitro* cultured HeLa cells. Cells were seeded at a density of 2×10^4 cells per well in a 24 well plate. 1 mL of complete high glucose DMEM (HG-DMEM with 10% fetal bovine serum, 1% penicillin and streptomycin, 1% L-glutamine) was used per well and incubated at 37 °C, 5% CO₂ for 24 h to adhere. Then, polymer samples of various concentrations in phosphate buffer saline (PBS, pH 7.4) containing 0.5% DMSO were added. The cells were incubated for another 48 h. At the same time, control cells and PBS control cells were incubated for the same time period. 100 µL of MTT from a stock solution of 5 mg/mL in PBS was added to each well of the 24 well plates and incubated for 4 h. Next, the culture media was discarded, and the resulting formazan crystals were dissolved in 500 µL DMSO. After 10 min, the absorbance was measured at 570 nm. The percentage of cell viability was calculated using the following equation:

$$\% \text{ cell viability} = (\text{Mean OD}_{\text{sample}} / \text{Mean OD}_{\text{blank}}) \times 100$$

where OD = optical density of the respective samples or blank.

Dynamic light scattering. For nucleation monitoring, a 2 µM stock solution of actin was prepared in G-buffer and incubated with 1 mM MgCl₂ and 10 mM ethylene glycol-bis(β-aminoethyl ether)-*N,N,N',N'*-tetraacetic acid (EGTA) for 2 min at room temperature. Various concentrations of the desired compound dissolved in HEK buffer (20 mM HEPES pH 7.5, 1 mM EGTA and 50 mM KCl) were then added, and the volume was adjusted with G-buffer and HEK buffer. Just prior to the polymerization reaction, 20X initiation mix (1 M KCl, 40 mM MgCl₂, 10 mM adenosine triphosphate (ATP)) was added. The final volume of the solution

was kept at 1 mL and placed in a dynamic light scattering (DLS) cuvette for experimentation. For stabilization monitoring, the 7.0 μM G-actin was polymerized in F-buffer (10 mM Tris-Cl pH 8.0, 0.2 mM dithiothreitol (DTT), 0.7 mM ATP, 50 mM KCl, 2 mM MgCl_2). The time course of depolymerization of 7.0 μM actin filaments after dilution to 0.25 μM was recorded with various polymers.

Circular dichroism spectroscopy. The change in the secondary structure during the nucleation and stabilization of G-actin was examined using circular dichroism (CD) spectroscopy, where the experimental solution concentrations were kept alike in the DLS study.

Table S1. Experimental results from the RAFT polymerization of Boc-Ala-HEMA and MAECA in DMF at 70 °C for 5 h using BBHT as CTA.

Polymer ^a	MAECA content in feed	Conv. ^b (%)	MAECA content in polymers ^c	$M_{n,theo}$ ^d (g/mol)	$M_{n,SEC}$ ^e (g/mol)	\mathcal{D} ^e	$M_{n,NMR}$ ^f (g/mol)
pCA0	00	74	00	11700	14500	1.21	12400
pCA2	02	70	2.1	10900	14600	1.17	13900
pCA4	04	66	5.1	10500	13700	1.17	12800
pCA8	08	68	8.8	11200	13900	1.27	13400

^aMAECA conjugated copolymers were synthesized using BBHT. ^bDetermined by gravimetric analysis on the basis of the amount of monomer feed. ^cDetermined from ¹H NMR analysis.

^d $M_{n,theo} = \{([Monomer]/[CTA] \times \text{average molecular weight (MW) of monomer} \times \text{Conv.}) + (\text{MW of CTA})\}$. ^eMeasured by SEC. ^fCalculated by ¹H NMR from the integration ratio of the repeating unit protons to that of the polymer chain end protons.

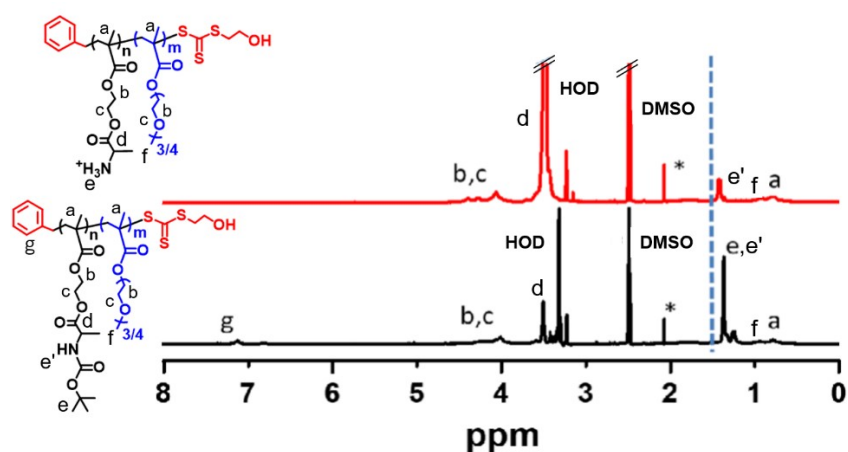


Fig. S4 The ^1H NMR spectra of P(PEGMA-*co*-Boc-Ala-HEMA), i.e., **pPA** (below) and the corresponding Boc deprotected copolymer P(PEGMA-*co*-Ala-HEMA), i.e., **PA** (above) in DMSO- d_6 .

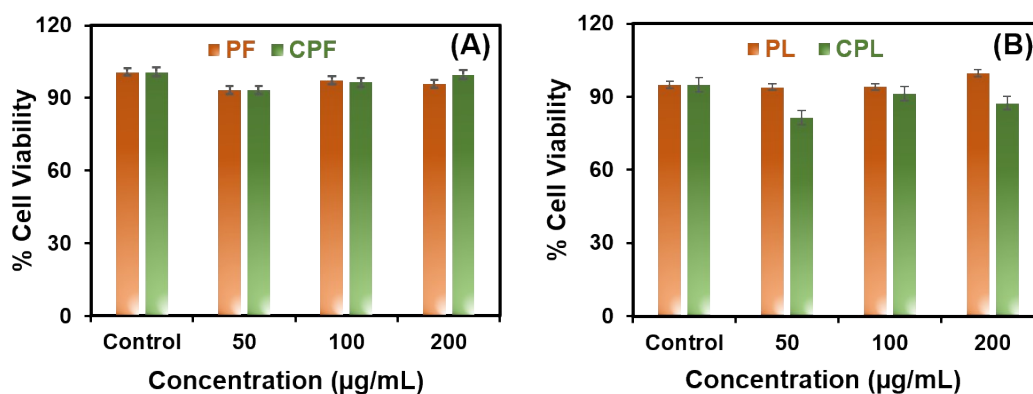


Fig. S5 % Cell viability vs polymer concentration profile of HeLa cells after treating with (A) **PF**, **CPF**, and (B) **PL**, **CPL** for 48 h followed by MTT assay. For each polymer, the mean value of three different data sets is shown through bar height, and the error bar indicates the maximum variation of the three values from the mean one.

Table S2. Zeta potential values of the different homo- and copolymers in aqueous media.

Polymer	Zeta potential (mV)
PA	$+20.4 \pm 3.4$
CPA	$+17.7 \pm 4.2$
PF	$+12.5 \pm 3.5$
CPF	$+13.4 \pm 2.9$
PL	$+21.0 \pm 3.1$
CPL	$+19.5 \pm 4.2$
CA0	$+35.5 \pm 3.8$
CA2	$+29.6 \pm 3.2$
CA4	$+30.9 \pm 4.0$
CA8	$+27.2 \pm 3.7$

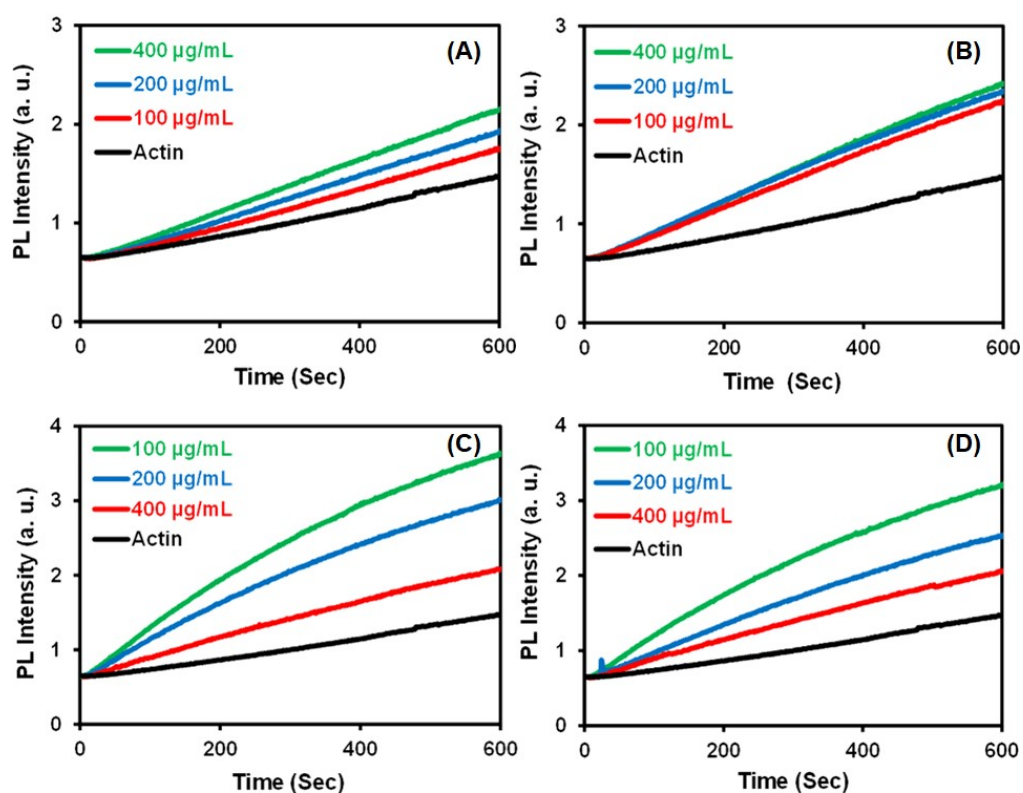


Fig. S6 Concentration-dependent polymerization of G-actin to F-actin by (A) PF, (B) CPF, (C) PL, and (D) CPL, compared with the pyrene-actin polymerization assay in the absence of polymer. For *in vitro* kinetics, 2 μM actin (10% pyrene labeled) was used.

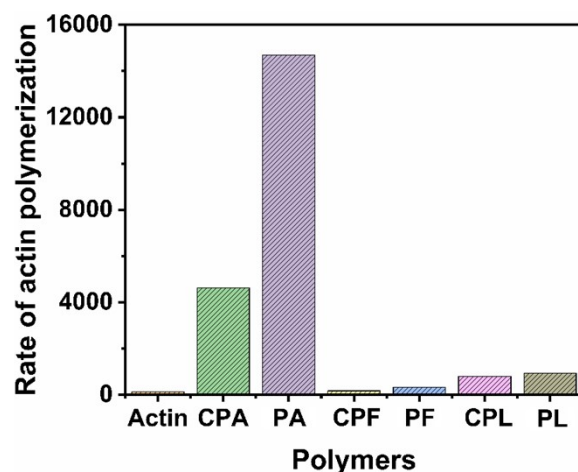


Fig. S7 Plot showing the different slope of nucleation for the PEGMA conjugated polymer induced actin polymerization; determined at 10-100 sec time phase. Nucleation assay was accomplished with 2 μM of 10% pyrene labeled actin. Polymer concentration was 400 $\mu\text{g}/\text{mL}$ in each case.

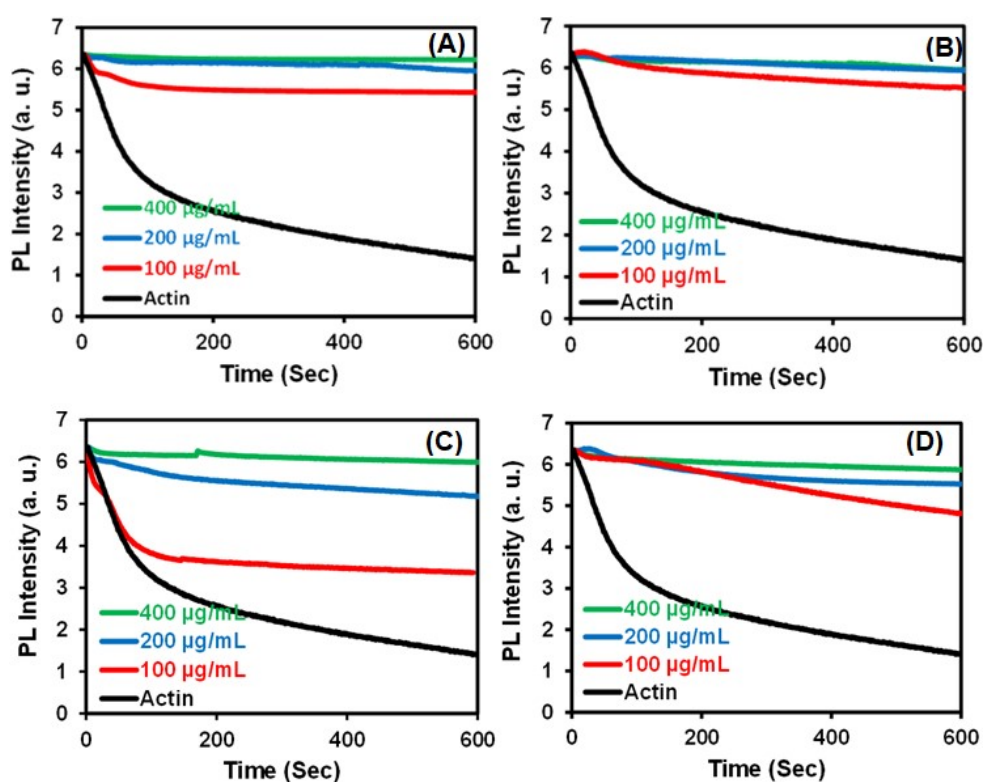


Fig. S8 (A) PF, (B) CPF, (C) PL, and (D) CPL induced stabilization of 0.25 μM of 10% pyrene labeled F-actin filaments with increasing polymer concentrations.

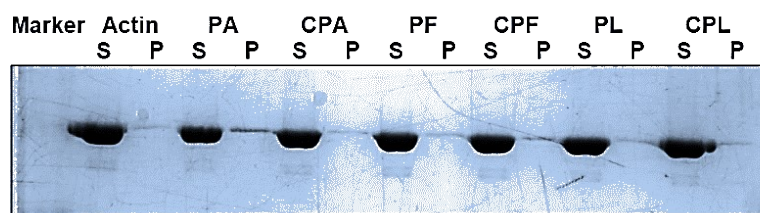


Fig. S9 Image of 12% SDS-PAGE of samples from low-speed actin co-sedimentation assay where 400 $\mu\text{g/mL}$ polymer (**PF**, **CPF**, **PL**, **CPL**) was incubated with pre-formed 5 μM F-actin for 20 min at 25 $^{\circ}\text{C}$ and centrifuged at 10000 RPM for 10 min. S: Soup, P: Pellet. For relevant comparison, results for **PA** and **CPA** are provided in the same image. See Fig. S21 for the raw images.

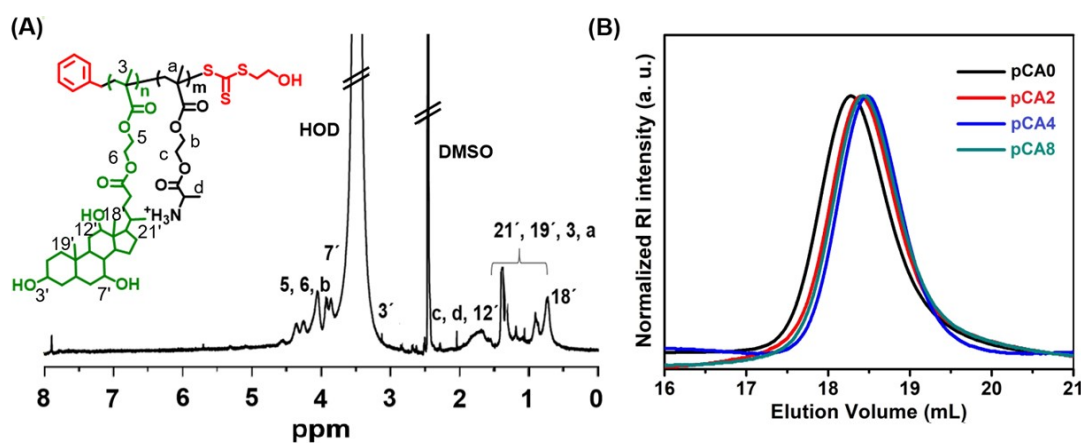


Fig. S10 (A) ^1H NMR spectrum of CA8 in $\text{DMSO-}d_6$. (B) SEC chromatograms of **pCA x** ($x = 0, 2, 4, 8$) polymers in DMF.

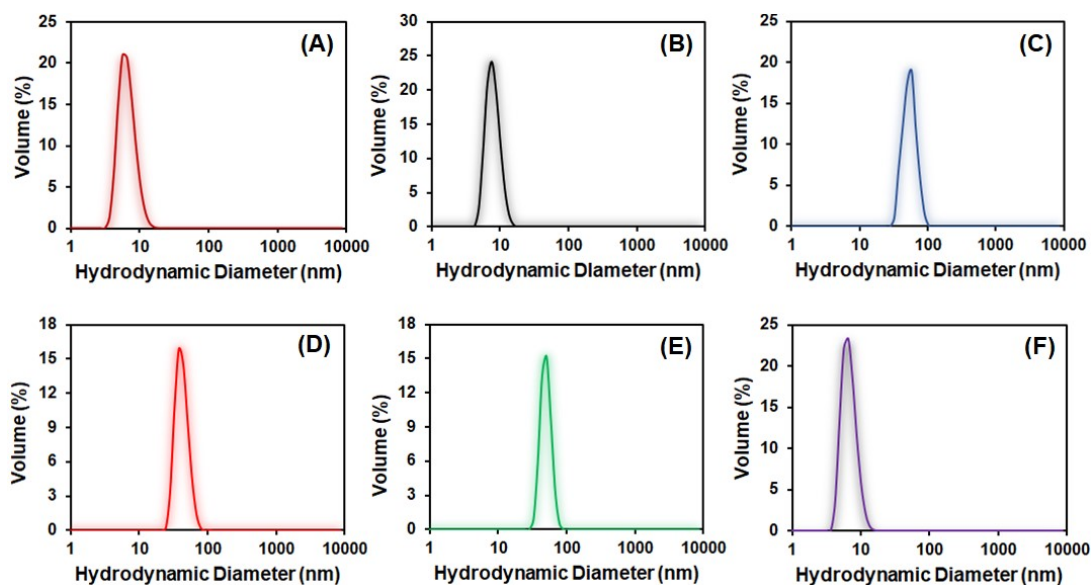


Fig. S11 Hydrodynamic diameter curves of (A) CPA, (B) CA0, (C) CA2, (D) CA4, and (E-F) CA8 in HEK buffer. Polymer concentration for A-E = 1 mg/mL, for F = 10 μ g/mL.

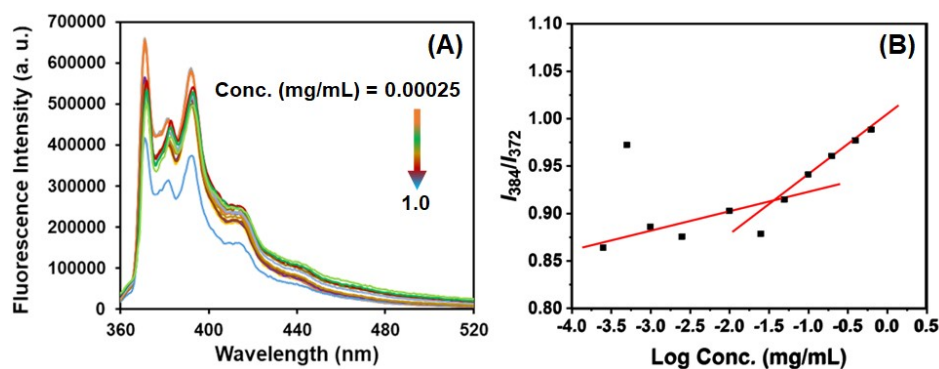


Fig. S12 (A) Pyrene emission spectra at different concentrations of CA8 in HEK buffer solution. (B) Plot of the intensity ratio (I_{384}/I_{372}) against the logarithmic concentration of CA8.

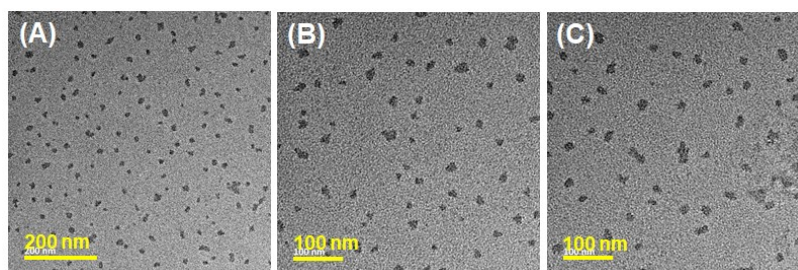


Fig. S13 TEM images of the self-assembly form the side-chain cholates conjugated polymers (A) CA2, (B) CA4, and (C) CA8 in buffer solution. Polymer concentration = 0.1 mg/mL.

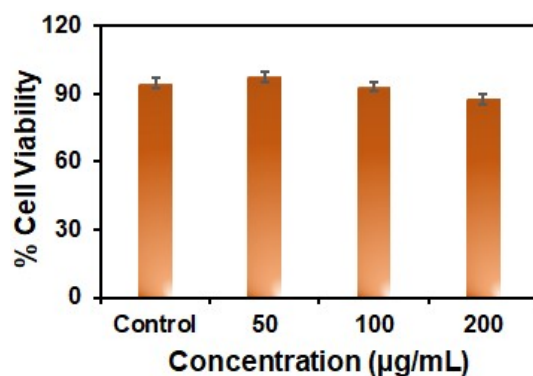


Fig. S14 % Cell viability vs polymer concentration profile of HeLa cells after treating with CA2 for 48 h following MTT assay. The mean value of three different data sets is shown through bar height, and the error bar indicates the maximum variation of the three values from the mean one.

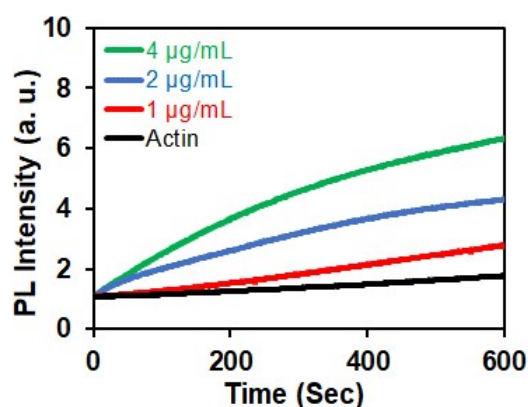


Fig. S15 CA4 induced nucleation of 2 µM pyrene labeled (10%) G-actin to filamentous F-actin with increasing polymer concentration from 1 to 4 µg/mL.

Actin Bundling. Actin filaments can crosslink together in presence of certain cross-linking proteins and form filament bundles that are thicker and heavier than actin filaments. It can occur in various formats such as tightly packed parallel bundles, loosely packed contractile bundles, or a web-like assembly; depending upon the type of protein associated with it. Several actin-bundling proteins such as fimbrin, α -actinin, spectrin, villin, fascin are identified to be associated with actin bundles inside cells.^{4,5} These structures are of immense importance for

stress fiber and contractile ring formation; for protrusion formation in specialized structures like microvilli in epithelial cells of the small intestine, neuronal growth cone and in general cellular filopodia formation.⁶

During *in vitro* low-speed actin co-sedimentation assay for actin bundle, the reaction mixture was centrifuged at 10000 RPM which is sufficient to pellet actin bundles but not the individual actin filaments. If any bundling occurs due to incubation with the target molecule, actin would be detected in the pellet fraction (Figure S16). In our case, actin was detected in pellet fraction with **CAx** polymers (**CA0**, **CA2**, and **CA8**) in a concentration-dependent manner (Figure 4E-G). This depicts the comparison between the bundling activity by **CAx** polymers. Nevertheless, the densitometric analysis of band intensity was performed using ImageJ/Fiji software version 1.8.0. The percentage of actin in the pellet fraction, which is directly proportional to bundle formation, was calculated and plotted against the polymer concentration (Figure S17). Error bars represent the standard deviation from three experiments. The percentage was calculated using the following equation:

$$\% \text{ actin in pellet} = \frac{I_{\text{actin in Pellet fraction}} - I_{\text{actin in 0 mg/mL polymer pellet fraction}}}{I_{\text{actin in pellet + supernatant}}} \times 100$$

'*I*' in the equation depicts the band intensity of the respective samples measured for densitometric analysis.

Therefore, it can be concluded from this result that **CA2** exerted the highest actin-bundling activity among all tested polymers and it saturated at 40 $\mu\text{g/mL}$ concentration which was again lowest than that of the other polymers.

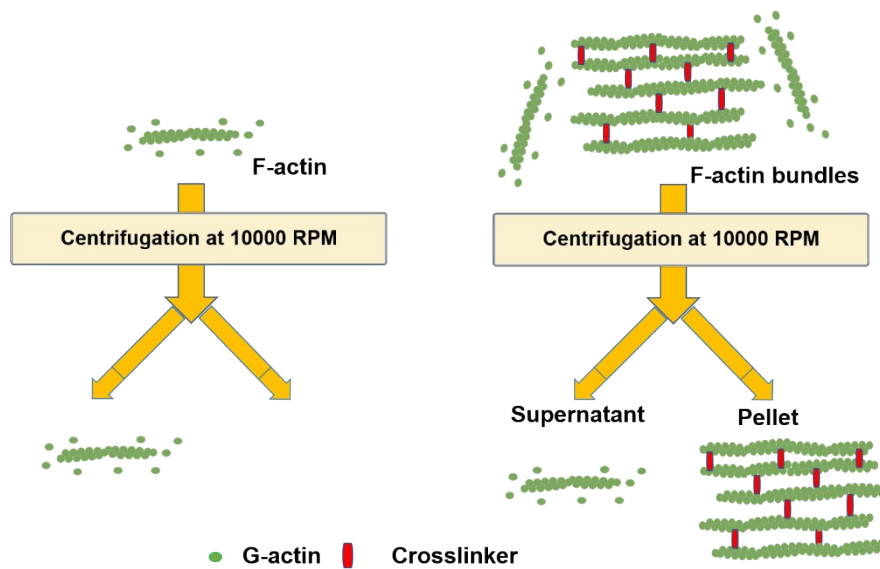


Fig. S16 General schematics of low speed actin co-sedimentation assay for extracting F-actin bundles *via* centrifugation process.

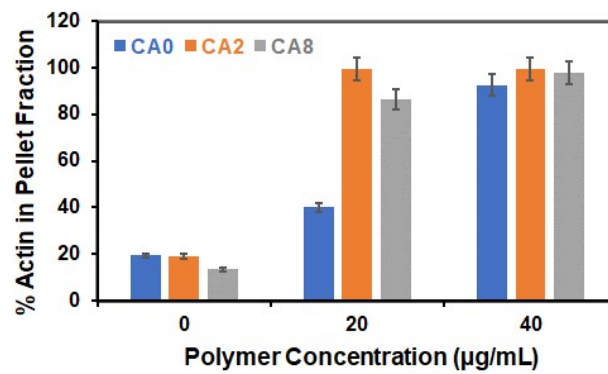


Fig. S17 Plot of %actin in pellet fraction vs concentration of CA0, CA2, and CA8, obtained from the densitometric calculations of Fig. 4E-G.

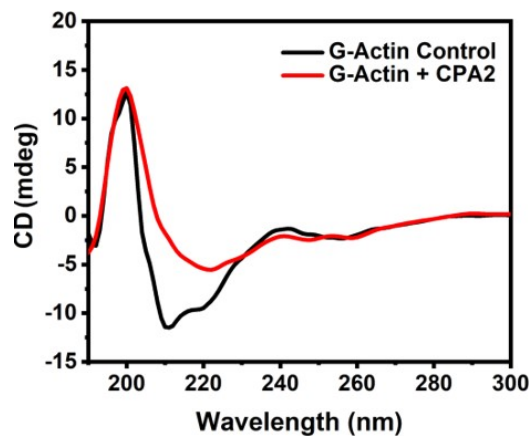


Fig. S18 CD spectra of 0.1 µM G-actin in the absence and presence of CA2.

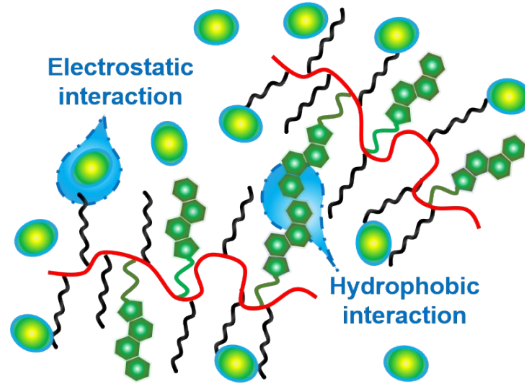


Fig. S19 Schematics of operational hydrophobic and electrostatic interactions in CA x ($x = 2, 4,$ and 8) polymers in the presence of monomeric G-actin upon immediate mixing.

Theoretical Model: Calculation of steady-state value,
$$N_S = V \left(C - \frac{K_{off}}{K_{on}} \right)$$
 in the case when only G-actin is present in the solution. In the experiment, the total volume, $V = 10^{-3}$ L; the effective concentration of free available actin monomer is $C = fC_0$, where $C_0 = 2 \times 10^{-6} M \approx 12 \times 10^{17}$ number of monomers/Litre (as 1 M contains 6.022×10^{23} constituent particles). In the presence of only G-actin, $f = f_0 = 0.30$. The values of $K_{off}^0 = 2.2 s^{-1}$ and $K_{on}^0 = 12.9 \mu M^{-1} s^{-1}$. Plugging in all these experimental parameter

values,

$$N_S = V \left(C - \frac{K_{off}}{K_{on}} \right) \approx 10^{14}$$

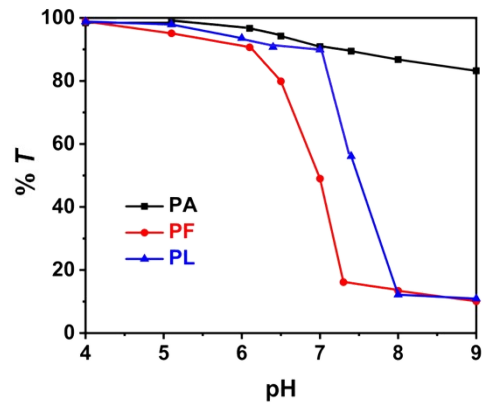


Fig. S20 Phase transition of PA, PF, and PL at different pH values at 25 °C.

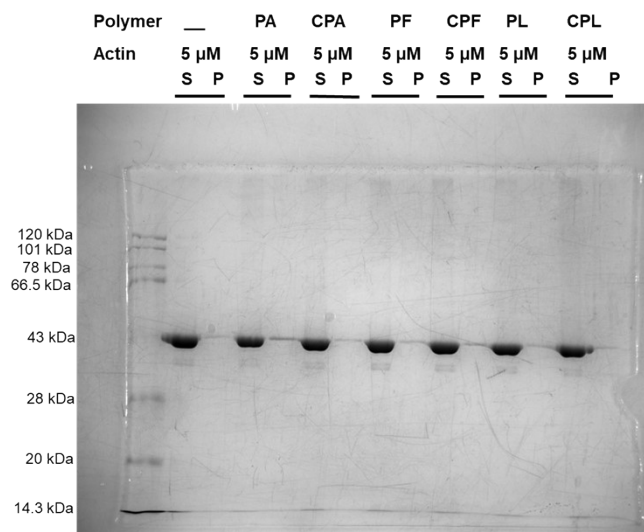


Fig. 21 Raw unprocessed image of 10% SDS-PAGE corresponding to Fig. S9A and Fig. 2F (The marker ladder is on left).

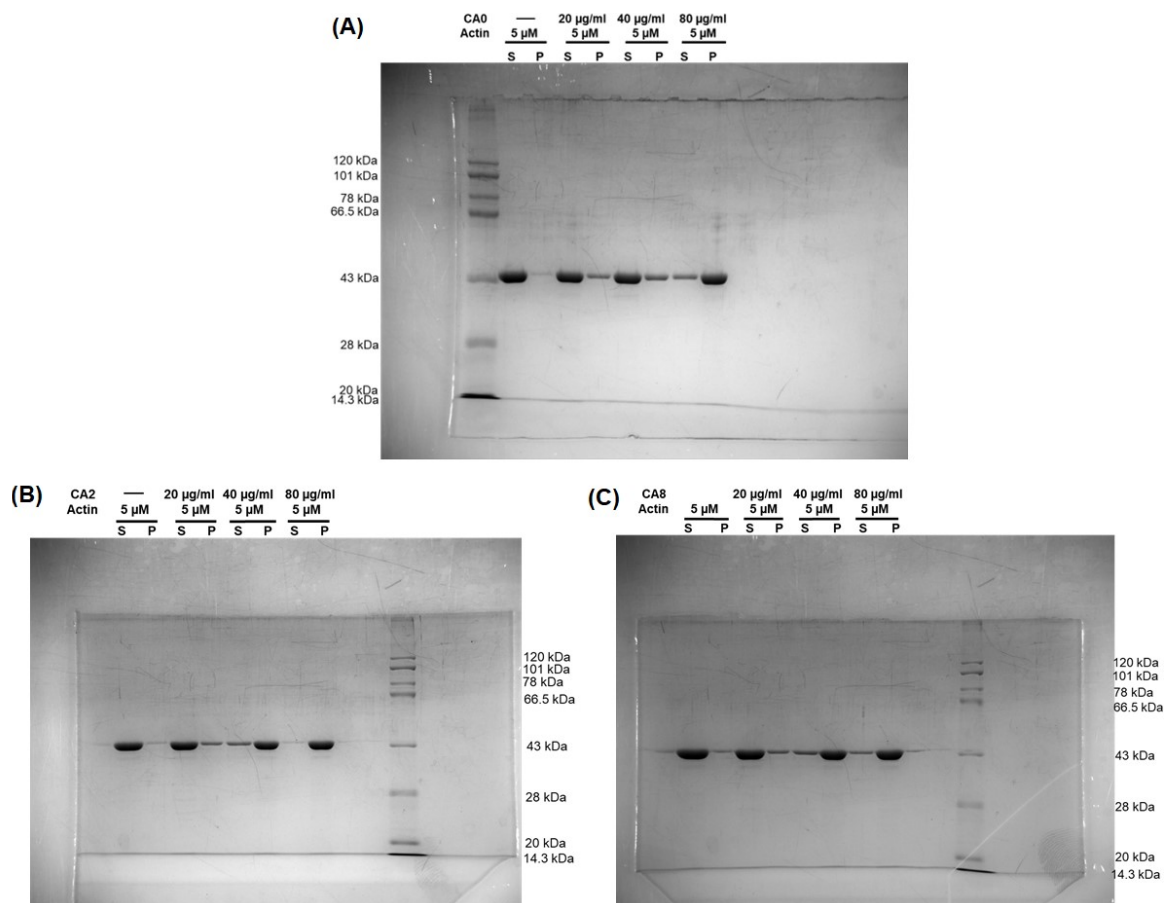


Fig. 22 (A-C) Raw 10% SDS-PAGE images corresponding to Fig. 4E-F respectively. Marker ladders are on left for Fig. S22A and on right for Fig. S22B-C.

References

- (1) S. Pal, S. G. Roy and P. De, *Polym. Chem.*, 2014, **5**, 1275-1284.
- (2) B. S. Furniss, A. J. Hannaford, P. W. G. Smith and A. R. Tatchell, in *Vogel's Textbook of Practical Organic Chemistry*, Longman Scientific & Technical Co-published in the United States with John Wiley & Sons, Inc., New York, 5th edn., 1989.
- (3) I. Mukherjee, A. Ghosh, P. Bhadury and P. De, *Bioconjugate Chem.*, 2019, **30**, 218-230.
- (4) J. R. Bartles, *Curr. Opin. Cell Biol.*, 2000, **12**, 72-78.
- (5) A. Li, J. C. Dawson, M. Forero-Vargas, H. J. Spence, X. Yu, I. König, K. Anderson, L. M. Machesky, *Curr. Biol.*, 2010, **20**, 339-345.
- (6) R. P. Stevenson, D. Veltman, L. M. Machesky, *J. Cell Sci.*, 2012, **125**, 1073-1079.